B. G. Huth
M. R. Kagan

Dynamics of a Flashlamp-pumped Rhodamine 6G Laser*

Abstract: In this paper a rate-equation model is developed for a single-wavelength dye laser. The model is unique in that it accounts for the fact that triplet-state lifetimes are not necessarily very long, as has been previously assumed. This modification makes it possible to analyze more accurately the behavior of dye lasers that are pumped with pulse energies above threshold. Computer solutions of the rate equations are obtained and an experimental technique is developed to measure amplifier gain, which is then used to estimate populations of molecules at various energy levels. An experimental study of triplet lifetimes in anthracene is included in an Appendix. These results support the experimental values obtained by Stockman for Rhodamine 6G, which are used in our calculations.

Introduction

Several analyses of the dye laser are available in the literature. Weber and Bass[1] and Snavely and Peterson[2] calculate gain as a function of wavelength for various combinations of parameters. These papers are interesting because they incorporate the large spectral bands of the molecules in the analysis, but their theories are not valid above threshold. Sorokin et al.[3] have presented a normalized rate-equation model for a single-wavelength dye laser pumped above threshold by a Gaussian-shaped flashlamp pulse. However, they assumed an infinite triplet state lifetime and concluded that a critical risetime existed for a flashlamp pulse. It is now known that dissolved oxygen and other compounds present in solution effectively quench the triplet state and make Sorokin's assumption of very long triplet lifetimes generally invalid. The use of chemical additives to deliberately quench triplet states is relatively new, and several materials that do this have now been reported[4].

In this paper we compare the theoretical results obtained from a rate-equation model with the performance of an actual dye laser operating in the laboratory. The rate equations include the dynamics associated with both singlet and triplet states. The flashlamp pulses that drive the system of differential equations are taken from experimental data at various pump energies; the computer solutions result in values for the populations of the various energy levels and give the laser output as a function of time. An effort is made to present the results in terms of meaningful laboratory parameters such as power and energy.

The rate equations are developed in the first section. An ancillary experiment for the measurement of gain is described in the second section. The third section of the paper includes the computer solutions to the rate equations and the experimental results for comparable conditions. A short study of the triplet lifetime of anthracene in several air-equilibrated solutions is given in Appendix A.

1. Dye laser model

The energy levels of an organic molecule are represented by the modified Jablonski diagram in Fig. 1. In general, the energies of the vibrational-rotational bands in the electronic states are functions of the coordinates of the atoms comprising the molecules. Since the dye molecules are usually very large, it becomes difficult to determine the energies analytically and, for the purposes of illustration, we assume that the states are a function of a single generalized coordinate, which is the abscissa in each of the two parts of the figure. The fact that the coordinate corresponding to the minimum energy is different for each group of states indicates that the equilibrium value of the generalized coordinate depends on the electronic state of the molecule. The Franck-Condon principle states that radiative transitions tend to occur between those vibrational-rotational levels of two electronic states for which the generalized coordinate is the

*This work was sponsored by the United States Air Force Avionics Laboratory, Wright Patterson Air Force Base, Ohio, under contract F33615-69-C-1296.

same, and, furthermore, transitions tend to take place at the turning points in each vibration where the nuclear kinetic energy is a minimum. These tendencies explain the Stokes shift of the fluorescence and are indicated in Fig. 1 by the different lengths of the solid lines representing absorption and emission in the singlet manifold. Excess energy is taken up by nonradiative transitions that are represented by the wavy lines.

In order to write a set of rate equations that model the dye laser, we have simplified the energy level diagram as shown in Fig. 2. Note that only the energy of the levels is shown, and the value of the generalized coordinates has been eliminated. The states shown on the left are the singlet states and depict the 4-level nature of the dye laser. The triplet states are on the right-hand portion of the diagram.

The two relevant vibronic levels in the ground singlet state are assumed to be in thermal equilibrium, and the populations are in a Boltzmann distribution. This is taken into account by the factors α and β which sum to unity and have the proper exponential ratio to one another[5]:

$$\beta = \frac{\exp\ (-\Delta E/kT)}{1 + \exp\ (-\Delta E/kT)}, \tag{1}$$

where ΔE is the energy between the vibronic levels.

The population density of the ground state is labeled N_1. It is assumed that optical pumping takes place between the ground state and the level with population density N_3. The molecules then undergo nonradiative transitions to the upper lasing level with population N_2.

Molecules can decay from the upper lasing state by fluorescence with a rate K_f. They can also decay nonradiatively by processes collectively called "internal conversion" K_{IC}, and the molecules can, in addition, cross over into the triplet manifold. This latter process is referred to as "intersystem crossing" and occurs at a rate K_{ISC}.

The fluorescence decay time, τ_f, is defined by

$$K_f + K_{IC} + K_{ISC} = 1/\tau_f \tag{2}$$

and the fluorescence quantum yield is

$$\Phi = K_f/(K_f + K_{IC} + K_{ISC}). \tag{3}$$

Molecules in the triplet manifold decay nonradiatively to the lowest triplet state which has population N_T and is metastable because of selection rules for transitions to the ground state. Radiative decay to the ground state can be observed as phosphorescence but usually has a very long lifetime. Nonradiative decay is much more likely and is caused by a number of possible quenching mechanisms. As mentioned in the Introduction, oxygen dissolved in solution is a very efficient quencher and is undoubtedly the most important mechanism.

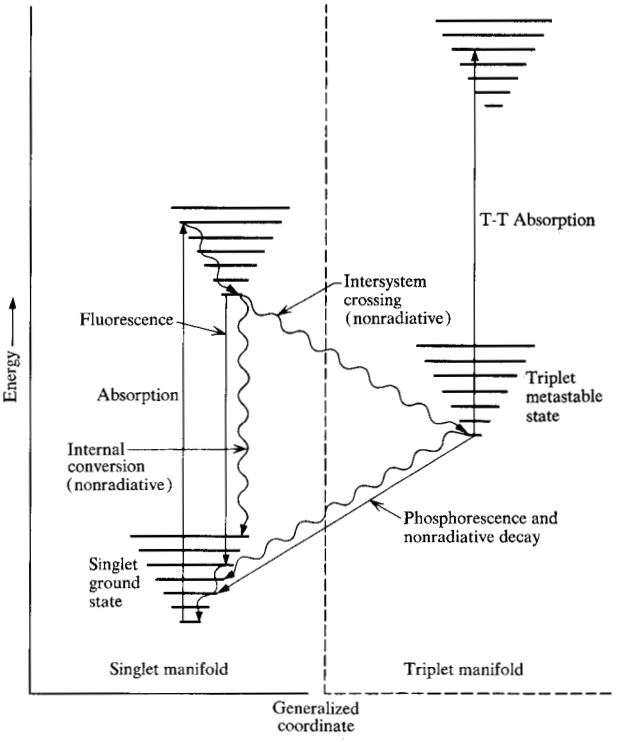

Figure 1 Typical energy-level (Jablonski) diagram for an organic molecule. The allowed energies are plotted as a function of a generalized configuration coordinate for the singlet and triplet states.

Figure 2 Energy-level diagram used to model the organic dye laser. The rates and other parameters are described in the text.

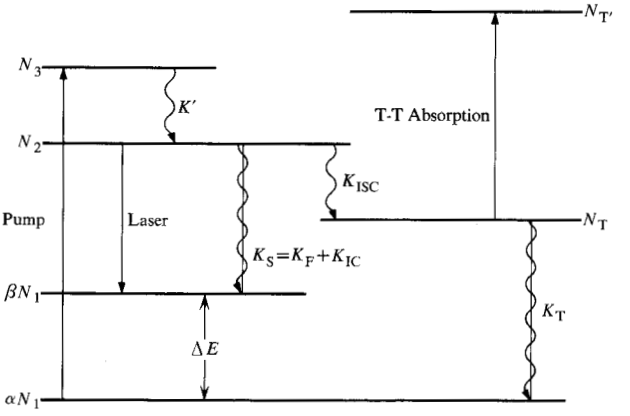

Those molecules temporarily in the metastable triplet state can also absorb radiation in a transition to higher triplet states. This absorption usually covers a broad spectral region which unfortunately overlaps parts of the fluorescence emission and, therefore, can represent an optical loss to the laser. In addition, molecules in the trip-

let state cannot produce laser emission as long as they are "trapped" in the metastable level. Stockman realized both of these difficulties with triplet states even before the first dye laser was in operation[6].

In spite of these potential problems, many dye lasers are operated successfully. The extent of the hindrance to laser operation depends on the magnitudes of the various rates and, as outlined in the Introduction, the purpose of this paper is to investigate the specific case of the dye Rhodamine 6G.

The rate equations for dye lasers whose energy levels are shown in Fig. 2 are given below.

$$\frac{dN_3}{dt} = \sigma_{SS'} c q_p \left[\alpha N_1 - N_3\right] - K' N_3, \tag{4a}$$

$$\frac{dN_2}{dt} = K' N_3 - \frac{q_L}{\tau_c F \Delta N_c}\left[N_2 - \beta N_1\right] - \frac{N_2}{\tau_f}, \tag{4b}$$

$$\frac{dN_T}{dt} = K_{ISC} N_2 - \frac{N_T}{\tau_T}, \tag{4c}$$

$$\frac{dq_L}{dt} = \frac{q_L}{\tau_c}\left[\frac{N_2 - \beta N_1}{\Delta N_c} - 1\right] - \frac{q_L}{\tau_c}\frac{N_T \sigma_{TT'}}{\Delta N_c \sigma_L}, \tag{4d}$$

$$N_1 + N_2 + N_3 + N_T = N. \tag{4e}$$

There is a differential equation for each of the levels except the ground state. Equation (4e), which requires the conservation of molecules, makes one differential equation redundant, and we choose to ignore the equation for the ground state. The population of the ground state can, of course, be calculated at any instant of time from the algebraic expression in (4e). The laser photon density is q_L. The equation for the photon density implies that the various parameters are relatively constant across the lasing band, and the transition is homogeneously broadened.

The pump photon density is q_p, the pump cross section is $\sigma_{SS'}$, ΔN_c is the critical inversion density determined in the absence of losses derived from the triplet states, and τ_c is the cavity lifetime. A filling factor is given by $F = L_{dye}/L_{cav}$, where the L's are lengths of the dye cell and the optical resonator. The lifetime of the triplet metastable state is τ_T and $\sigma_{TT'}/\sigma_L$ is the ratio of the triplet-triplet absorption cross section at the laser wavelength to the laser cross section. The total number of molecules per cm^3 is denoted by N. One can identify most of the terms in the equations by inspection of Fig. 2. The last term in (4c) accounts for the decay of the triplet metastable state and the last term in Equation (4d) represents the optical loss introduced by excited state absorption in the triplet manifold.

The power output from the mathematical model can be computed from

$$P_o = \frac{\text{Energy stored in cavity}}{\text{Coupling lifetime}}, \tag{5}$$

where the "coupling lifetime" refers to a cavity lifetime that includes only those coupling or loss mechanisms that contribute to the useful output. Since the coupling is normally accomplished with partially reflecting mirrors, this lifetime can be calculated from

$$\tau_o = \frac{L_{cav}}{c}\frac{\sqrt{\rho}}{1-\rho}. \tag{6}$$

In this equation c is the speed of light and ρ is the geometric mean of the two mirror reflectivities, i.e., $\rho = (R_1 R_2)^{1/2}$. In terms of the variables, the output power is, therefore,

$$P_o = h c q_L L_{cav} A_{cav} / \lambda_L \tau_c \tag{7}$$

with A_{cav} equal to the laser cross-sectional area.

Relating the pump power to the variables in the model is more difficult because of the lack of precise knowledge of spectral and geometrical coupling factors in actual laboratory devices. We can proceed with an idealized picture that can provide interesting results within the bounds of the necessary assumptions. Evtukhov and Neeland considered the problem of a "line" source and a laser material in the shape of a rod placed at the two foci of a polished elliptical cylinder[7]. By using their results one can relate the optical pump power in the source to the pump photon density in the laser dye.

It is useful to consider the steady-state solutions or quasi-steady-state solutions of (4a)–(4e.) If the time derivatives are set equal to zero and the resulting algebraic equations are solved under the assumption that $K' \gg \sigma_{SS'} e q_p$, the following expression for q_L is obtained:

$$q_L = \frac{F \Delta N_c (\tau_c/\tau_f)(\beta + \Delta N_c/N)}{\Delta N_c/N + \beta\xi} \times \left[\left\{\frac{(1-\xi)(\sigma_{SS'} c q_p)}{(\tau_c/\tau_f)(\beta + \Delta N_c/N)}\right\} - 1\right], \tag{8}$$

where

$$\xi = \frac{\Delta N_c}{N} + K_{ISC}\tau_T\left(\frac{\Delta N_c}{N} + \frac{\sigma_{TT'}}{\sigma_L}\right). \tag{9}$$

In most cases of interest, the constant ξ can be further simplified to the approximate value

$$\xi = K_{ISC}\tau_T(\sigma_{TT'}/\sigma_L). \tag{10}$$

Equation (8) is valid only above threshold. Note that the first term in the square brackets must be positive and greater than unity to produce laser emission. This term can never satisfy these requirements unless the positive definite constant ξ has a value less than one. Thus, steady-state operation of a dye laser is possible only if

$$\xi < 1. \tag{11}$$

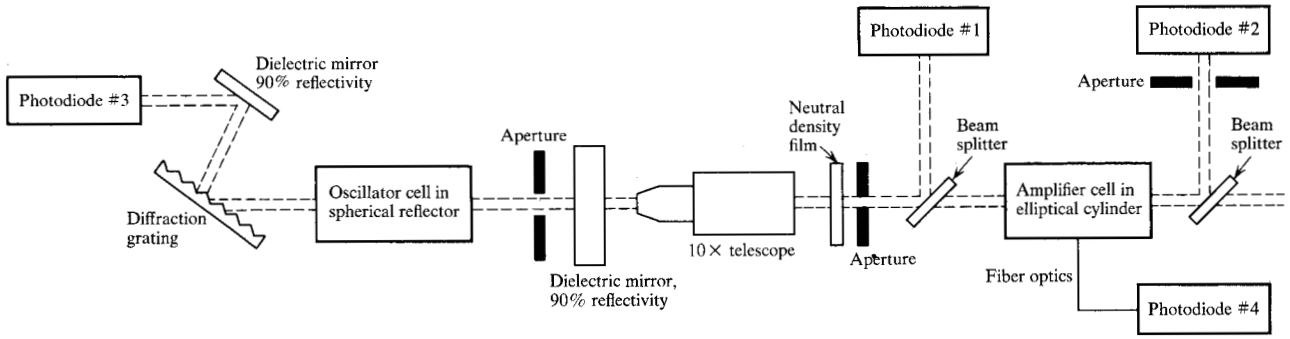

Figure 3 Apparatus for the gain measurements in Rhodamine 6G/ethanol.

The fact that a steady-state solution can exist contradicts the earlier analyses of dye lasers and leads to the possibility of CW operation[8] which recently has been experimentally achieved[9].

Laser operation when $\xi > 1$ is not precluded, but the results given above indicate that the solutions are transient in nature. In fact, when $\xi > 1$, one can show that a critical risetime for the flashlamp does exist by following the reasoning of Sorokin et al.[3].

The effects of dissolved oxygen can be included in the rate equations. It is well known that some molecules can quench the fluorescence and phosphorescence of organic compounds. Dissolved oxygen arising from contact with the atmosphere is an effective quencher, and the quenching reaction is diffusion controlled. In normal dye laser situations, oxygen quenching is the dominant process for relaxation of the triplet metastable state, and the triplet lifetime τ_T, can be written

$$\tau_T = 1/K_{O_2}[O_2], \tag{12}$$

where K_{O_2} is a rate constant and $[O_2]$ is the molar concentration of dissolved oxygen[10]. A brief derivation of dissolved oxygen concentration is given in Appendix B.

Oxygen can also quench the excited singlet state, presumably by increasing the intersystem crossing[11]. Thus the intersystem rate becomes

$$K_{ISC} = K^0_{ISC} + \eta K_{O_2}[O_2], \tag{13}$$

with η equal to the ratio of the singlet quenching rate constant to the triplet rate constant. This increased intersystem crossing reduces the singlet decay time which is described in a Stern-Volmer equation,

$$\tau_f = \tau_f^0/1 + \eta\tau_f^0 K_{O_2}[O_2], \tag{14}$$

where τ_f^0 is the singlet decay time in the absence of quenchers.

To apply the model presented in this section, one must know a value for the triplet decay time at dye concentrations that are typical for laser applications. Stockman has successfully measured the triplet lifetime of Rhodamine 6G in methanol in an apparatus capable of resolving changes of absorption on the order of one percent[12]. He has observed decay times between 90 and 120 ns.* Our own experiments in anthracene, described in Appendix A, support his results and show that triplet lifetimes in air-equilibrated solutions are approximately 10^{-7} s.

2. Gain measurements on Rhodamine 6G

To apply the rate equations to an actual laser, one must determine the magnitude of the pump term. This is, in general, a problem because it involves an electrical-to-optical conversion factor and optical coupling factors that are difficult to measure. We have adjusted the pump term in Eq. (4a) by an indirect method involving the single-pass gain. First the single-pass gain was measured in an oscillator-amplifier experiment. Next, the populations of the singlet and triplet states were obtained by fitting a theoretical curve of gain vs wavelength to the experimental data. The theoretical curve was generated from measured absorption and emission data. Finally, the pump term was adjusted in magnitude to produce these populations at the peak of the flashlamp pulse.

Figure 3 is a schematic diagram of the oscillator-amplifier apparatus used for the measurements[14]. The oscillator consisted of a cell 3.8 cm long with inside diameter 0.3 cm and a Xenon Corporation model 715 flashlamp mounted symmetrically in an 8-in. spherical reflector. Laser pulse durations of 400 ns were typical. A diffraction grating controlled the oscillator wavelength and reduced the laser bandwidth to approximately 1Å. An aperture was placed inside the laser resonator to improve the mode pattern and prevent stray reflections

*A value of 250 ns for the triplet lifetime in an ethanol solution has been reported[13]. This value is derived from the methanol data by calculating the concentration of dissolved oxygen and using the inverse dependence of the quenching rate constant with viscosity. Our results for anthracene show that this inverse dependence does not necessarily hold for low-viscosity solvents, and, therefore, this value for the triplet lifetime is suspect.

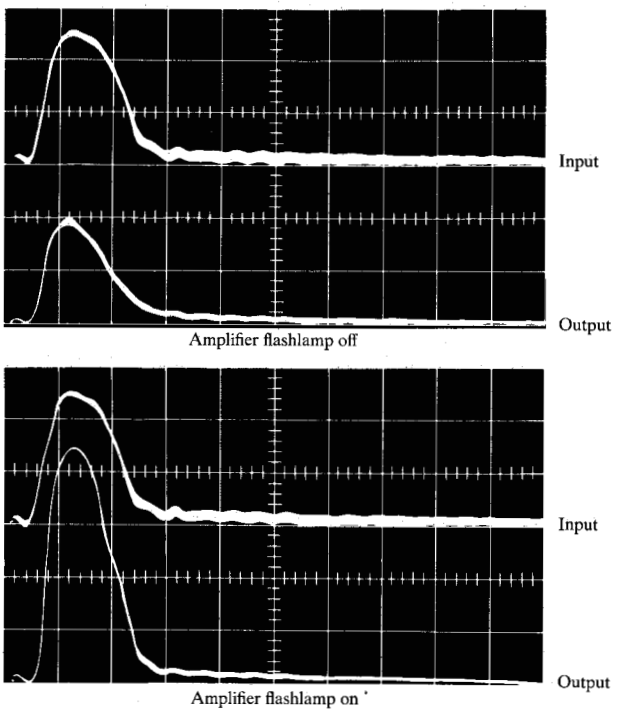

Figure 4 Typical oscilloscope traces of the amplifier input and output. The upper photograph shows the input and output from the amplifier with the flashlamp turned off. The lower photograph shows the same signals with the amplifier flashlamp in operation and clearly demonstrates the amplifier gain.

from the cell windows from entering the amplifier. The beam passed through a 10× beam-expanding telescope, a neutral density filter, and a 3-mm diameter aperture. The peak light intensity entering the amplifier was typically 20 W/ cm².

The amplifier cell was 3.8 cm long with 0.53 cm inside diameter and had antireflection-coated windows with 30-minute wedges. An EG&G FX-33C-1.5 flashlamp placed in an elliptical cylinder with an eccentricity of 0.27 was used to pump the amplifier. This flashlamp had a risetime of 3 μs and a halfwidth (FWHM) of 8 μs.

Two HPA 4203 PIN photodiodes were used to monitor the input and output of the amplifier. A representative oscilloscope display of the input and output signals is given in Fig. 4, with and without the amplifier flashlamp in operation. The amplifier gain may be seen very clearly. The delay between the oscillator and amplifier flashlamp discharges was adjustable, and the relatively short duration of the oscillator output pulse with respect to the amplifier pump pulse enabled the gain to be measured as a function of time. Two additional diodes monitored the oscillator output and the amplifier flashlamp pulses to assure proper synchronization.

Gain measurements were made by first recording a series of output and input pulses on a dual beam oscilloscope with the amplifier turned off and then calculating the ratio of the diode responses. Next, the ratio of output to input was determined with the amplifier flashlamp operating. Finally, the gain and the exponential gain coefficient were calculated from the quotient of these two ratios.

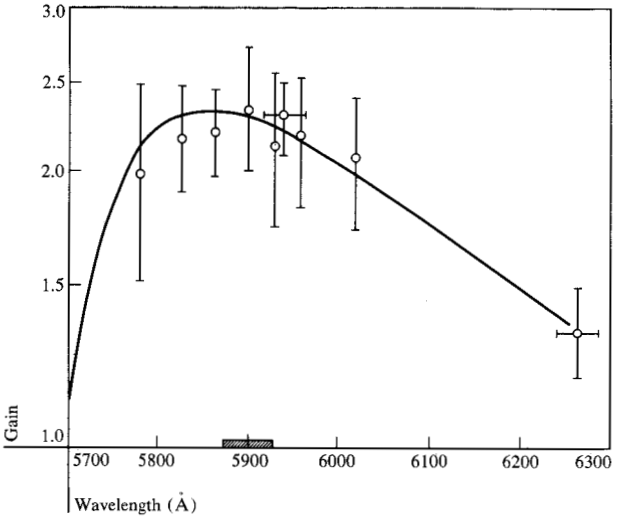

Figure 5 Gain as a function of wavelength for Rhodamine 6G/ethanol. The dye cell was 5.3 mm ID × 3.8 cm long. Input energy to the flashlamp was 21.5 J and the ethanol concentration was 2×10^{-4} M.

Figure 5 shows the peak gain as a function of wavelength for a 2×10^{-4} M solution of Rhodamine 6G/ethanol. Maximum gain for the 3.8 cm cell was 2.3, or, equivalently, the maximum gain coefficient was 95 dB/m. The input energy for this set of data was 21.5 J and the flashlamp synchronization was adjusted to measure the gain at the peak of the amplifier pulse. Similar measurements on a 5×10^{-5} M solution yielded a maximum gain of 1.4, or a gain coefficient of 38 dB/m.

The data points with horizontal error bars in Fig. 5 resulted from measurements with the diffraction grating replaced by a dielectric coated mirror. For this arrangement, the oscillator bandwidth was approximately 50 Å. These experimental results show that the small-signal gain is the same for broad-band and narrow-band light, and are consistent with the observation that the spectral condensation achieved with a diffraction grating takes place without a serious loss of laser output[15].

The solid curve in Fig. 5 was calculated from the gain expression[16]

$$G(\lambda) = \frac{I}{I_0} = \exp\left[N\left\{\frac{N_S}{N}\left[\frac{\lambda^4 E(\lambda)}{8\pi\tau_f c n^2} + \sigma_{SS'}\right] - \sigma_{SS'} - \frac{N_T}{N}\left[\sigma_{TT'} - \sigma_{SS'}\right]\right\}\right], \quad (15)$$

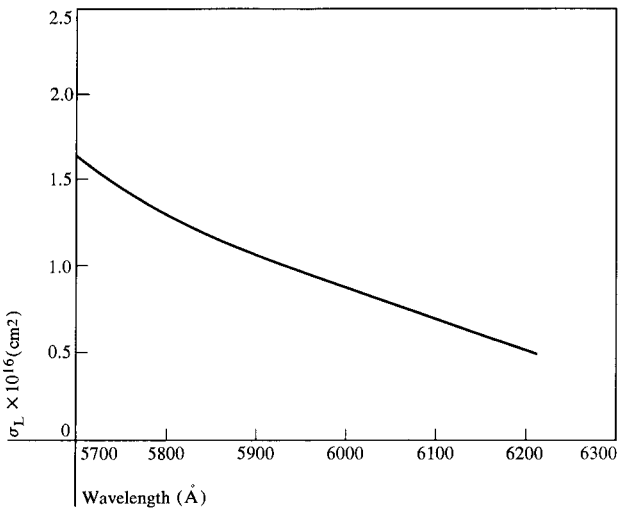

Figure 6 Laser cross section σ_L as a function of wavelength. This was determined from the fluorescence spectrum using the first term in Eq. (15).

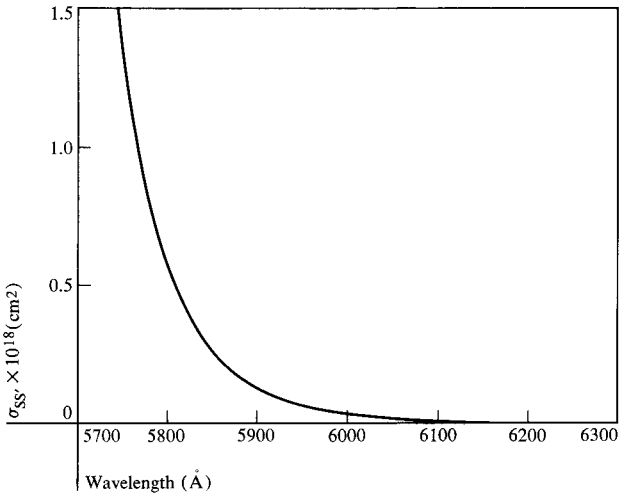

Figure 7 Absorption cross section as a function of wavelength for Rhodamine 6G/ethanol. This was measured on a Cary 14 spectrophotometer using a 10-cm cell.

where N, N_S, N_T are the total number of molecules and the numbers of molecules in the singlet and triplet states, respectively. $\sigma_{SS'}(\lambda)$ and $\sigma_{TT'}(\lambda)$ are singlet and triplet cross sections and τ_f is the fluorescence decay time. $E(\lambda)$ is the fluorescence spectrum normalized so that $\int E(\lambda)\, d\lambda = \Phi$, where $\Phi = 0.84$ is the quantum yield. The fluorescence spectrum, $E(\lambda)$, was measured in the laboratory, and the laser cross section, $\sigma_L(\lambda)$, derived from it is shown in Fig. 6.

The triplet cross section, $\sigma_{TT'}(\lambda)$ was taken from Snavely's review paper[16]. Figure 7 shows the singlet cross section, $\sigma_{SS'}(\lambda)$, which was measured in our laboratory. Other values used in the calculation were: $N = 1.2 \times 10^{17}\,cm^{-3}$, $\tau_f = 5.5 \times 10^{-9}s$, and $n = 1.36$. The fractional population densities in the singlet and triplet states were used to fit the shape and magnitude of the theoretical gain curve to the experimental data. $N_S/N = 0.019$ and $N_T/N = 0.04$ were used to obtain the curve in Fig. 5. These numbers are in good agreement with the steady-state ratio of triplet to singlet populations for the case when the triplet decay time, τ_T, is limited to approximately 100 ns by oxygen quenching[12].

In an effort to correlate the measured small-signal gain and the resulting laser performance, a maximum reflectivity flat mirror and a 65% reflectivity mirror with a 1-m radius-of-curvature were placed along the amplifier axis and separated by 30 cm. With the amplifier operated as a laser, a peak power of 2.2×10^4 W and an output energy of 55 mJ were obtained from the 2×10^{-4} M solution of 21.5 J input (the pump energy used for the gain measurements). The laser mode diameter was approximately 3.6 mm, and the emission spectrum was centered

Figure 8 Gain as a function of time for Rhodamine 6G/ethanol. (a) Time behavior of the amplifier flashlamp pulse, (b) measured gain at various times. The gain was measured at 5900 Å and the ethanol concentration was 2×10^{-4} M.

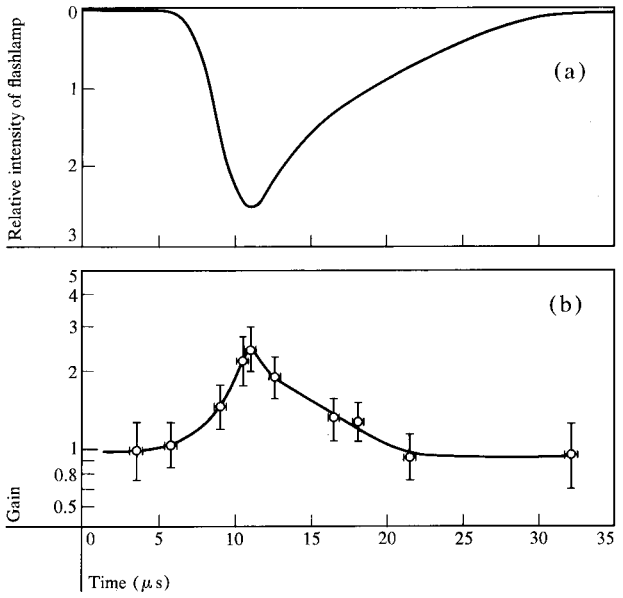

at 5900 Å as indicated by the shaded box in Fig. 5. Threshold occurred at 10 J, and an output energy of 131 mJ was obtained at 38.2 J input for an overall efficiency of 0.34% and a slope efficiency of 0.47%.

Figure 8 shows the amplifier gain as a function of time during the flashlamp pulse. One can see that gain exists for a significant portion of the flashlamp pulse, both be-

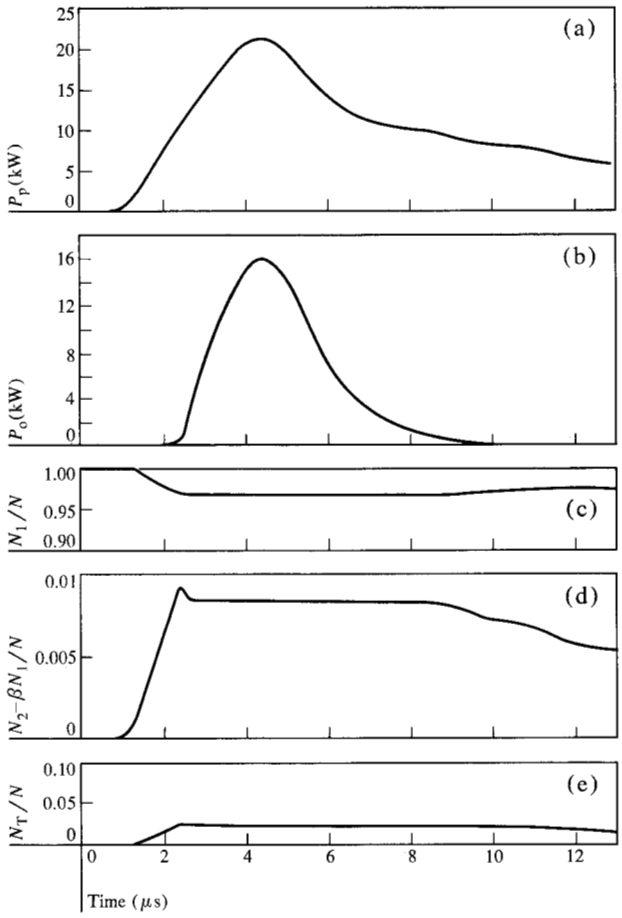

Figure 9 Results of the computer simulation for 21.5 J input. The following quantities are shown as functions of time: (a) pump power; (b) laser output power; (c) fractional ground state population; (d) fractional population inversion; (e) fractional triplet state population. Note that after threshold is reached, the laser is in a quasi-steady state, and the various populations are near their steady-state values.

Table 1 Parameter values used in computations of laser dynamics for the case of a 65% output reflector and a pump energy of 21.5 J.

$\lambda_L = 5890$ Å	$\tau_T = 100$ ns	$\sigma_L/\sigma_{TT'} = 19$
$L_{cav} = 30$ cm	$\tau_f = 5.5$ ns	$\Delta E = 1510$ cm^{-2}
$L_{dye} = 4$ cm	$\tau_o = 4.7$ ns	$K_{ISC} = 2.9 \times 10^7$ s^{-1}
$A_{cav} = 0.1$ cm^2	$\tau_c = 3$ ns	$\Phi = 0.84$

fore and after the peak. The long-pulse work of Snavely and Schafer[8,16] clearly demonstrated that the critical risetime criterion developed by Sorokin et al.[3] is not applicable to Rhodamine 6G/ethanol because dissolved oxygen in air-equilibrated solutions quenches the triplet states.

3. Computer solutions of rate equations

The solutions to Eqs. (4a) to (4e) were obtained numerically on an IBM 1800 computer and CalComp plotter. Actual flashlamp pulse shapes were digitized and served as the driving function for the Runge-Kutta integration routine. Interpolation between data points from the flashlamp pulse was done with a sliding-polynomial subroutine.

Results are given in this section for three pump energies and two different output mirror reflectivities. The shape of the flashlamp pulse changes with energy content, and the driving function for the computer solutions was changed accordingly. When the output mirror reflectivity in the model is modified, one must also change the values of several other parameters because the wavelength is dependent on the optical cavity Q. Thus the ratio of singlet and triplet cross sections, the critical inversion density, and the ground-state vibronic energy separation, ΔE, must all be adjusted.

To fix the magnitude of the pump term, as explained in the first paragraph of Section 2, the threshold in the model was artificially raised by increasing the critical inversion density to the point where the laser was below threshold. Next, the magnitude of the pump term was adjusted until the fractional number of molecules in the first excited singlet state was 0.019, and this value was considered to represent an input of 21.5 J. Scaling the pump to higher and lower input energies was based on the relative areas under the various pulse shapes.

For the case of a 65% output reflector and a pump energy of 21.5 J, the parameters in Table 1 were used in the model. The ground-state vibronic energy separation, ΔE, is determined by the ratio of the absorption cross section, $\sigma_{SS'}(\lambda)$, at the lasing wavelength to the maximum value of the cross section $\sigma_{SS'} = 3 \times 10^{-16}$ cm^2. K_{ISC} was calculated from Eqs. (2) and (3) with internal conversion ignored, and the cavity lifetime was deduced from changes in threshold observed when different output mirrors were used. This method for estimating the cavity lifetime is admittedly less than ideal since the changing Q causes a shift in wavelength and hence a change in single-pass gain, but the amplifier measurements indicate that the errors introduced are probably comparable with the uncertainties in most of the other parameters. The critical inversion density can be calculated from $\Delta N_c = 1/\sigma_L c F \tau_c$. Substituting the values given above and a value of $\sigma_L = 1.07 \times 10^{-16}$ cm^2 taken from Fig. 6, one calculates $\Delta N_c = 7.9 \times 10^{14}$ cm^{-3}.

Figure 9 shows the results of the computer calculations. The top trace gives the flashlamp pulse calibrated in kilowatts. Assignment of a power to the flashlamp is highly artificial but still interesting. We have assumed that all the pumping occurs at the peak absorption wavelength ($\lambda = 5300$ Å) where a decadic molar extinction

coefficient of 75,000 l/M-cm exists, and that the elliptical cylinder has perfectly reflecting walls and follows the analysis of Evtukhov and Neeland[7]. Therefore, under these highly restrictive assumptions, the pump power indicated is capable of creating the single-pass gains measured in the amplifier experiments.

The second trace is the laser output and has a peak power of 17 kW. Integration yields an output energy of 50.4 mJ, which is in excellent agreement with the experimental results. Integrated pump energy is 138.0 mJ, which indicates that perhaps as much as 99.35% of the actual 21.5-J input energy may be wasted.

The bottom three traces show the fractional ground-state population, the fractional population inversion, and the fractional triplet-state population. Approximately 3.2% of the molecules per cm^3 leave the ground state during the lasing process and the population inversion is clamped at 0.78% for the duration of the laser pulse. The triplet-state population is also clamped at its value when threshold occurs, which is, in this case, 2.4%.

The value of ξ for the parameters used is 0.15 and satisfies Eq. (11); hence, mathematically a steady-state solution exists. In fact, because the driving function changes only a small amount during the period of time equal to the longest decay time in the system of equations, namely $\tau_T = 100$ ns, the time derivatives are small with respect to the other terms in the equations, and the steady-state solution at any instant of time is in excellent agreement with the complete solution. The quasi-steady-state solutions are adequate for all times above threshold except during the time when the laser is turning on. During this period of time, solutions to the differential equations are necessary to obtain the small transient observed in the plot of population inversion shown in Fig. 9.

Another important point should be emphasized here. Early termination of dye laser pulses has been attributed to triplet-triplet absorption, even though the pulse duration is tens or hundreds of microseconds long before the cessation of lasing. It seems highly unlikely that this is the explanation for lasers using air-equilibrated solutions, because attempts at simulating this behavior with the model have yielded negative results unless the triplet lifetime was made artificially large.

Consider, for a moment, the sequence of events among the various levels as the pumping starts. Population in the upper laser level starts to grow. The population in the triplet metastable level also begins to grow, but through the process of intersystem crossing. The time constants of the singlet and triplet states are different, of course, and the population of the singlet state follows the pumping pulse more closely. There is a slight lag in the population of the triplet state because of the longer time constant. When the laser threshold is reached, the population of the singlet state is quickly clamped slightly

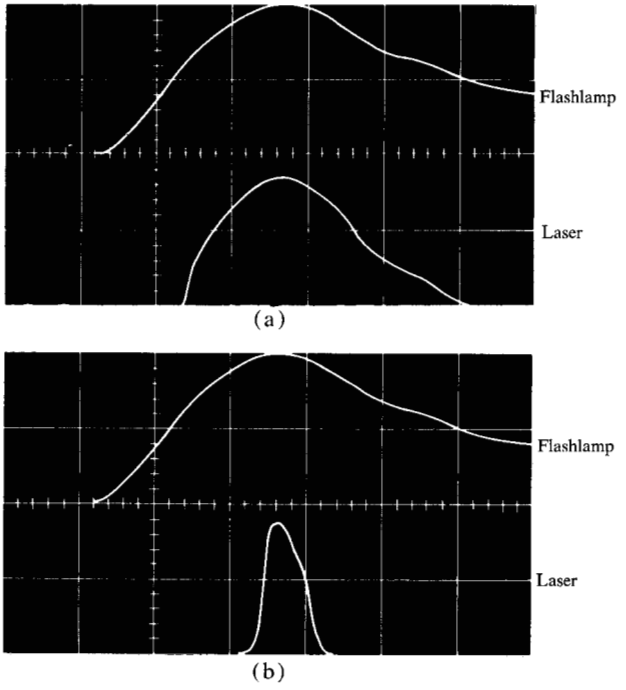

Figure 10 Computer simulation for mirror reflectivities of (a) 90% and (b) 65% for an input energy of 11.5 J. Note that the higher-Q resonator ($R = 90\%$) remains above threshold longer, as one would expect. The horizontal scale is 2μs/div and the vertical scales are not calibrated.

above its threshold value. After this point in time, the population of the triplet state approaches its steady-state value as determined by Eq. (4c) assuming a constant N_2. When this steady-state value of triplet population is reached (in several triplet decay times) the triplet-triplet absorption is at its maximum value. Thus, in the case of air-equilibrated solutions, triplet states would not be expected to increase the system losses after 200 to 600 ns. Since laser pulses have been observed with durations in excess of 140 μs in air-equilibrated methanol solutions[8], one must conclude that the triplet losses are not great enough to prevent initial laser action, and that since the duration is roughly three orders-of-magnitude longer than the estimated triplet lifetime, other mechanisms must be responsible for terminating the laser pulse.

The presence of triplet quenchers such as dissolved oxygen or other compounds certainly affects the magnitude of the triplet absorption and is manifested in the laser threshold, but the fact remains that if $\xi < 1$ and if threshold can be reached, the triplet population (and absorption) will approach a steady state that will limit the triplet loss to very near its value at threshold unless there is some additional time-dependent loss mechanism[17].

Figures 10(a) and 10(b) show simulations of the laser at 11.5 J input with output mirror reflectivities of 90%

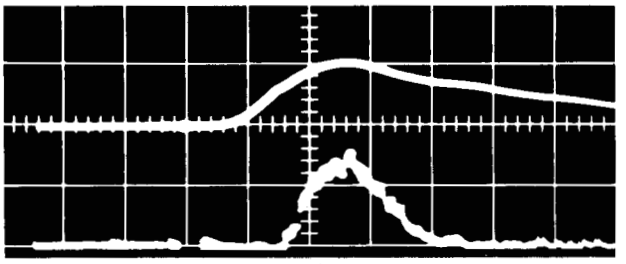

(a)

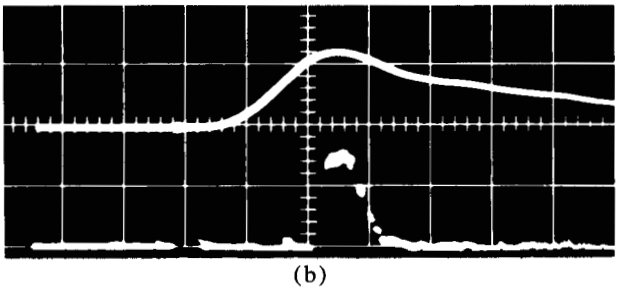

(b)

Figure 11 Photographs of the actual laser output for the same conditions as indicated in the caption for Fig. 10.

Table 2 Parameter values used in computation of laser dynamics for the cases of 65% and 90% output reflectivity with a pump energy of 11.5 J.

Parameters	*Parameter values*	
	Output reflectivity	
	90%	65%
λ_L	5960 Å	5890 Å
ΔE	1660 cm^{-1}	1510 cm^{-1}
ΔN_c	4.3×10^{14} cm^{-3}	7.9×10^{14} cm^{-3}
$\sigma_1/\sigma_{TT'}$	17	19
τ_c	6 ns	3 ns
τ_0	19.5 ns	4.7 ns

and 65%, respectively. The horizontal scale is 2 μs/div, and the vertical scale is not calibrated. Since changing the mirror reflectivity changes the laser wavelength, several parameters used in the computer solutions must be modified. Table 2 gives the parameter values for the two reflectivities. All other parameters are the same as those given in Table 1.

As one would expect, the solutions show that the higher reflectivity cavity comes above threshold at a lower pump level and produces a longer output pulse. Figure 11 shows the results obtained in the laboratory; there is good qualitative agreement between the two results.

The pulses shown in Fig. 12 represent the solutions for input energies of 11.5 J, 21.5 J and 38.2 J, with an

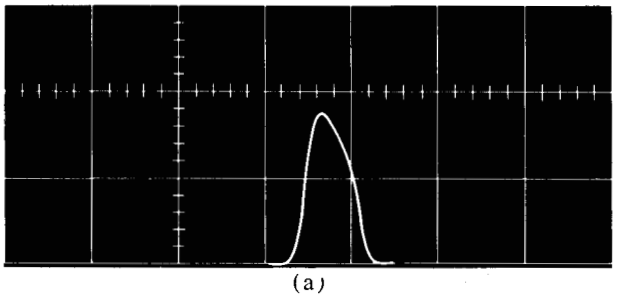

(a)

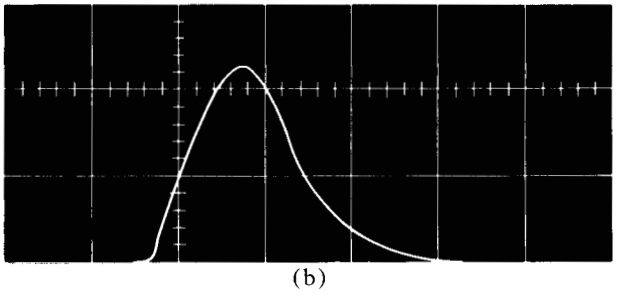

(b)

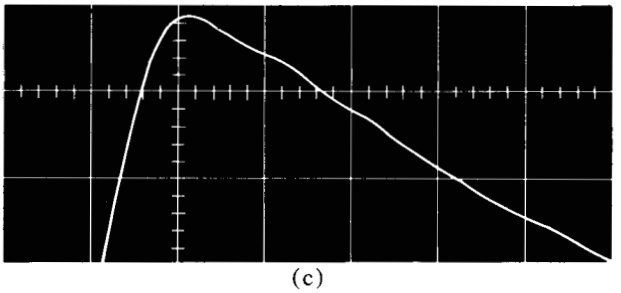

(c)

Figure 12 Computer simulation of laser output pulses for a mirror reflectivity of 65% and three different input energies; (a) 11.5 J, (b) 21.5 J and (c) 38.2 J. The horizontal scale is 2μs/div.

output reflectivity of 65 %. The pulse duration increases as the laser is pumped further above threshold, and the shape of the pulse becomes similar to that of the flashlamp pulse. Experimental counterparts to the three pulses are shown in Fig. 13. The shapes of the pulses agree quite favorably, once again, but it is evident that the calculated pulse at the highest energy is somewhat longer than the pulse observed experimentally.

Output energies for the model and the actual laser are given in Table 3. The experimental output data and two of the calculated energies are plotted in Fig. 14 as a function of the input energy.

It has been well established that when air-equilibrated solutions of Rhodamine 6G are degassed, the laser output is reduced or vanishes entirely. This situation has been investigated with the rate-equation model. In the computer solutions described above, Eqs. (12) to (14) have been used to determine the singlet and triplet decay times, and the intersystem crossing rate. The parameters used in those equations were $K_{O_2} = 6.67 \times 10^9$ 1/M-

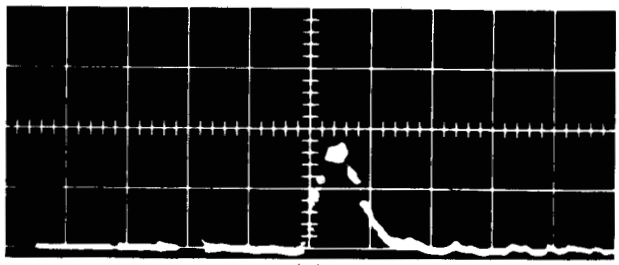

(a)

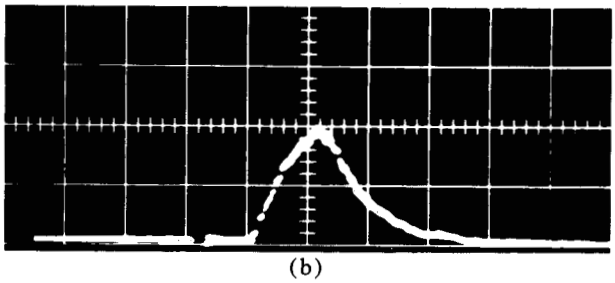

(b)

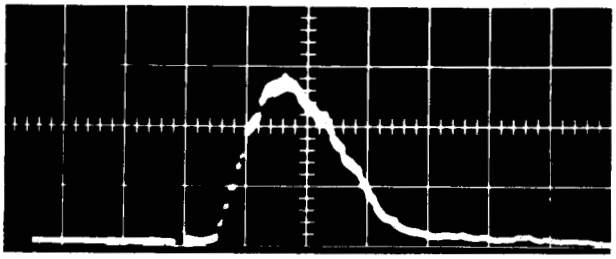

(c)

Figure 13 Photographs of the actual laser output for the same conditions as indicated in the caption for Fig. 12. Note that at the highest energy, the computer predicts a slightly longer laser pulse than is actually observed.

s, $[O_2] = 1.5 \times 10^{-3}$ M/1, $K^o_{ISC} = 1.8 \times 10^7$ s^{-1}, $\tau^o_f = 5.8 \times 10^{-9}$ s and $\eta = 1$. The whole system of equations can be modified systematically by changing the oxygen concentration.

The computer solutions for three concentrations of oxygen with a pump energy of 21.5 J are shown in Fig. 15. As the oxygen concentration is reduced, the pulse amplitude and width are reduced, as one would expect. In curve C, the laser is just barely above threshold. The time behavior of the various population densities is similar to those given in Fig. 9. A summary of various parameters is tabulated in Table 4 for the different oxygen concentrations.

These results seem to be in good qualitative agreement with experimental observation, but we can not claim any positive quantitative comparison because the rate constants are not well established. Because of this lack of data we have made two assumptions that could have important ramifications, namely, setting $K_{IC} = 0$ and $\eta = 1$. Keller[11] has investigated other values for η

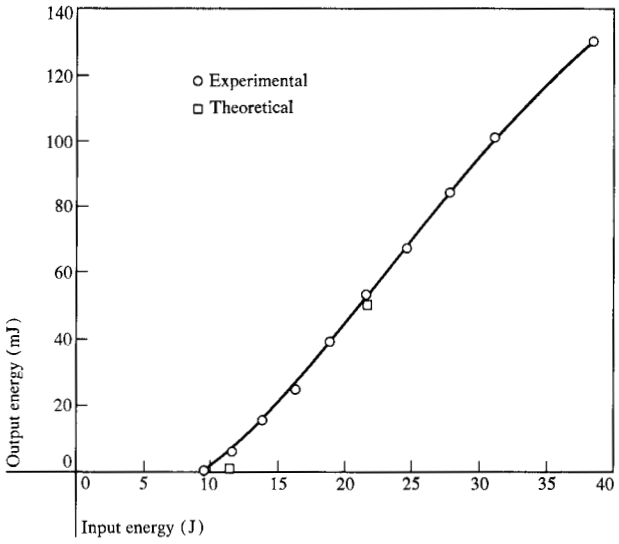

Figure 14 Plot of output energy vs input energy.

Table 3 Comparisons of calculated and experimentally determined output energies as functions of input energy.

	Output energy in milliJoules	
Input energy in Joules	*Calculated values*	*Experimental values*
11.5	1.0	6
21.5	50.4	55
38.4	180.0	131

Figure 15 Calculated laser output for an input energy of 21.5 J as the oxygen content of the solution is reduced. The O_2 concentrations assumed are $A = 1.5 \times 10^{-3}$ M, $B = 5 \times 10^{-4}$ M and $C = 2.5 \times 10^{-4}$ M. The horizontal scale is 2μs/div.

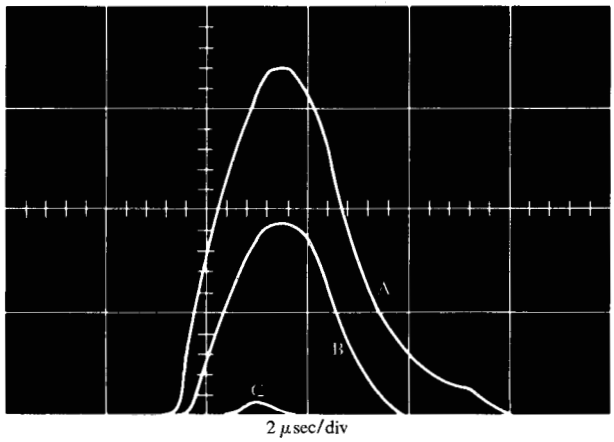

2 μsec/div

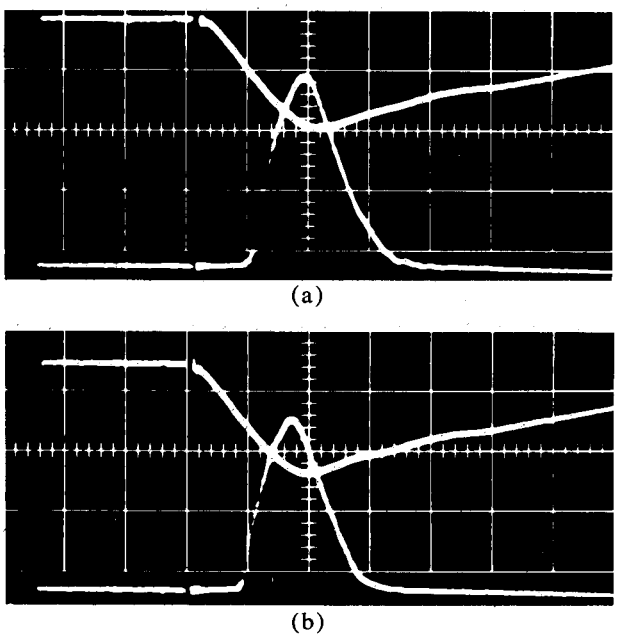

Figure 16 Laser output for 21.5 J input with two solvents: (a) methanol and (b) ethanol.

Table 4 The effect of oxygen concentration on laser dynamics. A pump energy of 21.5 J is assumed in the calculations.

Parameters	*Parameter values*		
	O_2 concentration in moles/liter		
	1.5×10^{-3}	5×10^{-4}	2.5×10^{-4}
τ_T	100 ns	300 ns	600 ns
τ_f	5.48 ns	5.69 ns	5.74 ns
K_{ISC}	2.8×10^7 s^{-1}	2.13×10^7 s^{-1}	1.97×10^7 s^{-1}
Φ	0.847	0.879	0.887
ξ	0.147	0.336	0.62
N_T/N^*	2.3%	6.9%	16%
P_{out}**	17.1 kW	9.5 kW	0.5 kW

*Evaluated at time of peak laser output.
**Peak laser output.

with one conclusion being that for some dyes the amount of oxygen present in air-equilibrated solutions may be very close to the optimum amount. If more oxygen is added in this situation, fluorescence quenching is sufficient to impair laser performance. In addition, the presence of large amounts of oxygen can cause oxidation and the formation of peroxides, so our results cannot be interpreted to mean that saturating the solutions with oxygen will improve laser performance.

The necessity of using methanol rather than ethanol for the production of long pulses as reported by Snavely[18] prompted a comparison of these solvents in our laser. One might expect better performance with methanol for two reasons. First, the fact that the viscosity of methanol is approximately half of that for ethanol could lead to more collisions between the dissolved oxygen and excited triplets. Second, the thermal properties of methanol are better than those of ethanol.

The laser output pulse with 21.5 J input for the two solvents is shown in Fig. 16. As one can see, the two pulses are nearly identical, which indicates that the change in viscosity does not introduce a significant change in the triplet lifetime. Such a change would have been manifested in a reduced threshold, and an increased pulse duration and output energy. This simple experiment does not give any information on the thermal effects because of the short duration of the flashlamp pulse.

4. Discussion and summary

In the previous three sections we have described a rate-equation model for a Rhodamine 6G dye laser and have identified usable values for the important parameters. The purpose of this study was not to infer the magnitude of dye parameters such as triplet lifetime and intersystem crossing rates, but instead to show that values within the bounds of a reasonable estimate can be used to predict the performance of a dye laser, and in addition, provide valuable insight into the laser dynamics.

Two points discussed in the earlier sections deserve to be re-emphasized. First, if the parameter $\xi = K_{ISC}\ \tau_T\ (\sigma_{TT'}/\sigma_L)$ is less than unity, steady-state solutions to the laser equations can exist. The possibility of steady-state operation was first recognized by Snavely and Schafer[8] and led to the construction of a CW dye laser[9]. As a corollary to this principle, if $\xi < 1$, triplet-triplet absorption cannot lead to early termination of the laser pulse since such an occurrence is contradictory to the definition of a steady-state solution. Our best estimates as given in Table 4 indicate that ξ is less than unity. In addition, the flashlamp pulse used in this paper violates the "critical risetime" criterion of Sorokin et al.[3], which for our parameter estimates, requires that the risetime should be less than 1.3 μs, and is, thus, one additional indication that long pulses are not precluded. Therefore, at least for air-equilibrated solutions, other mechanisms such as thermal distortion or more complicated photochemical processes must be considered in order to explain premature termination of long pulses.

The second point is that dissolved oxygen in solution is an excellent quencher of triplet states in most organic compounds. This oxygen is the result of an equilibrium between the solvent and the partial pressure of O_2 in the atmosphere, and the concentration may be calculated from solubility coefficients. Unless care is taken to degas the dye solvents, dissolved oxygen will undoubtly be present.

It is an interesting exercise to assemble the efficiency data from the simulations. Three pump levels are given in Table 5. The entries in the "electrical input energy" column are the three pump energies used in the laboratory comparisons and have been identified with corresponding sets of computer solutions by means of the gain measurements. The "usable optical energy" is the somewhat artificial pump energy obtained from the driving function for the differential equations under the assumptions of ideal ellipse and a narrow-band pumping source located at the wavelength of peak absorption in Rhodamine 6G. Electrical-to-optical efficiency, therefore, represents that fraction of the electrical energy that was necessary to generate the laser pulses, and is 0.65%. The fraction of light absorbed by the dye ("usable optical energy") and returned as laser output is labeled "optical-to-laser efficiency" and has a maximum value of 73%. It is obvious that the factor limiting the efficiency of the dye laser is the process of converting electrical energy to optical energy useful for pumping the laser medium.

One more piece of information may be extracted from the gain measurements presented above. This is the saturation intensity of Rhodamine 6G. The saturation intensity is the circulating power density in the laser necessary to reduce the population inversion to one-half its small-signal value. It also is an indication of the power levels necessary for the lasing process to compete favorably with spontaneous emission.

The output power of the laser is related to the saturation intensity, I_{sat} by the following equation.

$$P_{out} = I_{sat} A \frac{1-\rho}{\rho}(cF\tau_c g_o - 1), \tag{16}$$

where $\rho = (R_1 R_2)^{1/2}$, A is the area, and g_o is the unsaturated, small-signal gain coefficient. The output energy for the laser with 21.5 J input was 55 mJ and the base-width of the pulse was approximately 5 μs. If one makes a triangular approximation for the pulse shape, the peak output power is 2.2×10^4 W. The other parameter values necessary to evaluate the saturation intensity are as follows: $g_o = 0.22$ cm^{-1}, $\rho = (0.65 \times 1)^{1/2} = 0.806$, $F = 0.133$, $\tau_c = 3 \times 10^{-9}$ s and $A = 0.1$ cm^2. Upon substitution of these values into Eq. (16), one finds

$$I_{sat} = 6.2 \times 10^5 \text{ W/cm}^2.$$

An alternate expression for the saturation intensity is

$$I_{sat} = \hbar\omega/\tau_f \sigma_L. \tag{17}$$

The fluorescence lifetime for Rhodamine 6G is approximately 5.5 ns, and the laser cross section at 5900Å can be read from Fig. 6 as 1.06×10^{-16} cm^2. Substitution into Eq. (17) yields

$$I_{sat} = 5.8 \times 10^5 \text{ W/cm}^2.$$

Table 5 Computed efficiencies for several values of pump energy.

Electrical input energy	*Usable optical energy*	*Laser output energy*	*Electrical to optical efficiency*	*Optical to laser efficiency*	*Total efficiency*
11.5 J	76 mJ	1 mJ	0.66%	1.3%	0.0087%
21.5	139	50	0.65	36	0.23
38.4	248	180	0.65	73	0.47

To place this number in perspective, one may compare this result with the saturation intensities of other laser materials. In a transverse-flow CO_2 laser, $I_{sat} = 246$ W/cm^2[19] and in Nd:YAG, $I_{sat} = 720$ W/cm^2[20]. The saturation intensity for Rhodamine 6G is three orders-of-magnitude larger than those of the other materials, which implies that very large pump rates are required for efficient operation.

Appendix A: Triplet decay time measurements in anthracene

To apply the model presented in Section 1, one must know a value for the triplet decay time at concentrations that are typical for laser applications. We assembled a flash photocatalysis experiment to measure the decay time of a representative molecule. We would have preferred data on Rhodamine 6G, but the measurements on this dye are very difficult to make because of the large fluorescence quantum yield and the small triplet-triplet extinction coefficient. As a compromise, we chose to measure anthracene, which has a quantum yield of 0.36 and a peak triplet-extinction coefficient of 75,000 l/M-cm[21]. It is not unreasonable to expect the results with anthracene to be similar to those that would be obtained with other molecules since the rate of collision between the oxygen and the excited molecules is diffusion controlled.

The population of the triplet state, N_T, can decay back to the ground state through a variety of processes in fluid solution. Three important processes are represented by the terms on the righthand side of Eq. (a).

$$-\frac{dN_T}{dt} = [K_P + K_{O_2}[O_2] + K_{TT'}N_T]N_T, \tag{a}$$

where N_T is the concentration of triplets, $[O_2]$ is the concentration of oxygen and K_P is the rate arising from phosphorescent decay, $K_{O_2}[O_2]$ is the deactivation rate from collisions between dye molecules in the triplet state and oxygen molecules. $K_{TT'}N_T$ is the rate dependent on collisions between two excited molecules in the triplet state.

The radiative transition from the excited triplet state to the singlet ground state is forbidden, and therefore K_P

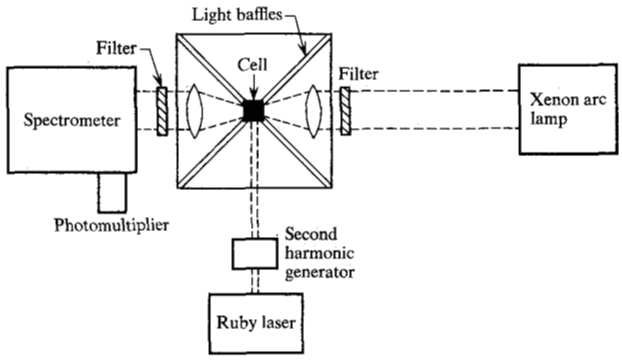

Figure A1 Diagram of the triplet lifetime experiment. The second harmonic of a ruby laser was used to excite the organic molecules. A xenon arc lamp was used to monitor the triplet-triplet absorption as a function of time.

Figure A2 Typical data from the triplet absorption experiment.

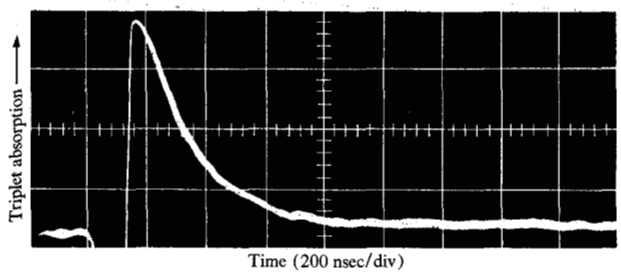

Figure A3 Reduction of data for anthracene in chloroform. The triplet lifetime is 135 ns.

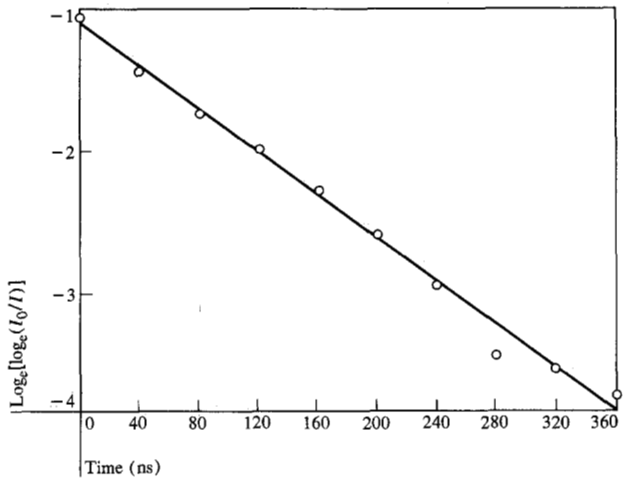

is relatively small ($K_P \approx 200\ s^{-1}$). Quenching reactions are known to be diffusion controlled, and the rate of reaction is determined by the frequency of collisions. This frequency is, in general, inversely proportional to the solvent viscosity[22]. Typical values for K_{O_2} and $[O_2]$ are 10^9 l/M-s and 10^{-3} M/l, respectively. Thus, the nonradiative quenching rate is approximately four orders-of-magnitude larger than the radiative decay. Triplet-triplet quenching will depend on the number of triplets generated, but for typical cases this quenching rate will be several orders-of-magnitude smaller than the rate for oxygen quenching.

Figure A1 shows the experimental apparatus for measuring triplet lifetimes. A beam of light from a xenon arc lamp passes through a cuvette and into a spectrometer. Second harmonic light from a ruby laser entered the cuvette 90° from the xenon beam and served to excite the material. The spectrometer adjustment and the filter passbands were chosen to be in the triplet-triplet absorption band.

The 20-ns pump pulse excites the molecules to the singlet and triplet states. The singlet states decay in only a few nanoseconds, but the excited-state triplet absorption continues for longer periods. Since the excited-state absorption is proportional to the population of the triplet metastable level, the triplet lifetime can be measured by monitoring the temporal behavior of the triplet-triplet absorption.

Figure A2 is a representative oscilloscope trace for anthracene. The spectrometer was set to 4220Å. Fluorescence from the anthracene drives the trace off scale on the bottom during the pump pulse. After the fluorescence is over, the triplet absorption dominates and gradually decays. We may extract the decay time from this data by considering the following.

The intensity of the xenon probe is attenuated according to

$$I = I_0 \exp\ (-\sigma_{TT'} N_T L), \tag{b}$$

where L is the path length illuminated by the pump and $\sigma_{TT'}$ is the triplet-triplet absorption cross section. In room temperature aerated solutions, we can approximate Eq. (a),

$$-dN_T/dt = K_{O_2}[O_2]N_T, \tag{c}$$

with the lifetime, τ_T, given by

$$\tau_T = 1/K_{O_2}[O_2]. \tag{d}$$

From Eqs. (b), (c) and (d), we find that

$$\log_e(I_0/I) = \sigma_{TT'} N_T L = \sigma_{TT'} L N_T{}^0 \exp(-t/\tau_T) \tag{e}$$

or

$$\log_e[\log_e(I_0/I)] = \log_e(\sigma_{TT'} L N_T{}^0) - (t/\tau_T). \tag{f}$$

Thus, the triplet lifetime is the inverse of the slope of $\log_e[\log_e(I_0/I)]$ plotted vs t. A set of data for anthracene in chloroform is given in Fig. A3. The points fit a straight line rather well and indicate a lifetime of 135 ns. At $t = 0$ (an arbitrary time chosen close to the maximum absorp-

tion) we can estimate the maximum concentration of triplets. For $\epsilon_{TT} = 75{,}000$ and $L = 0.65$ cm, $[N_T{}^0] = 3.1 \times 10^{-6}$M/1.*

Four solvents were investigated. The properites are given in Table A1. The triplet decay times for three concentrations of anthracene were measured and are tabulated in Table A2.

The constant, K_{O_2}, can be calculated from Eq. (d). Values derived from the information in Tables A1 and A2 are plotted in Fig. A4 as a function of viscosity. Normally, one expects K_{O_2} to be inversely proportional to viscosity[22]. However, our data show a more linear relationship. Keller has pointed out that the expected inverse dependence may be modified at low viscosities because the molecules diffuse apart before the quenching reaction can occur. He also points out that when the viscosity is greater than 3 cp, every collision results in energy transfer[11].

The data for methanol do not seem to follow the trend established by the other three solvents. In fact, the viscosities of chloroform and methanol are nearly the same, but the resulting values for K_{O_2} are significantly different. The explanation of the different behavior with methanol is not apparent, but the larger value is consistent with the observations of Schafer and Snavely that their long-pulse laser performed best with methanol solvent[18].

We have also considered degassed solutions. If the quencher concentration is small, but the triplet concentration high, Eq. (a) can be approximated by

$$-dN_T/dt = K_{TT}N_T{}^2. \tag{g}$$

This equation can be integrated:

$$-N_T = 1/[(1/N_T{}^0) + K_{TT}t]. \tag{h}$$

Substituting (h) into Eq. (b), we find

$$[\log_e(I_0/I)]^{-1} = [N_T{}^0\sigma_{TT'}L]^{-1} + t(K_{TT}/\sigma_{TT'}L) \tag{i}$$

Thus, when triplet-triplet collisions dominate the decay processes, a plot of $1/[\log_e(I_0/I)]$ vs time yields a straight line.

A solution of anthracene in methanol was degassed by the freeze-thaw technique. The results are shown in Fig. A5. The slope, $K_{TT}/(\sigma_{TT'}L)$, is 5.1×10^4. By substituting the values for $\sigma_{TT'}$ and L given above, we find,

$K_{TT} = 9.5 \times 10^{-12}$ cm^3/s.

In summary, we have investigated the triplet decay time in anthracene for several solvents. The decay times ranged from approximately 80 to 150 ns. These times are much shorter than expected from radiative decay rates and are a direct result of oxygen quenching present in aerated solutions. De-oxygenated solutions placed in our apparatus showed that the decay time was controlled by triplet-triplet collisions.

* $(\log_e 10)\epsilon_{TT'}[N_T{}^0]L = \sigma_{TT'}N_T{}^0L$. The molar extinction coefficient, $\epsilon_{TT'}$, is related to the cross section by this relation and Avogadro's number.

Table A1 Parameter values for selected properties of several solvents.

Solvent	*Viscosity in centipoise*	*Ostwald coefficient*	*Oxygen concentration in moles/liter*
Ethyl Ether	0.23	0.568	4.8×10^{-3}
Chloroform	0.58	0.451	3.8×10^{-3}
Methanol	0.60	0.247	2.1×10^{-3}
Ethanol	1.20	0.241	2.05×10^{-3}

Table A2 Triplet decay times for three concentrations of anthracene.

Solvent	*Decay times in ns*		
	Anthracene concentration in moles/liter		
	1.4×10^{-4}	2.8×10^{-4}	5.6×10^{-4}
Ethyl Ether	128	138	150
Chloroform	135	121	129
Methanol	81	85	78
Ethanol	85	123	135

Figure A4 Quenching constant as a function of solvent viscosity. Note that although methanol and chloroform have nearly the same viscosity, larger values of the constant were observed for the methanol solutions. Solvent concentrations are 2.8×10^{-4} M.

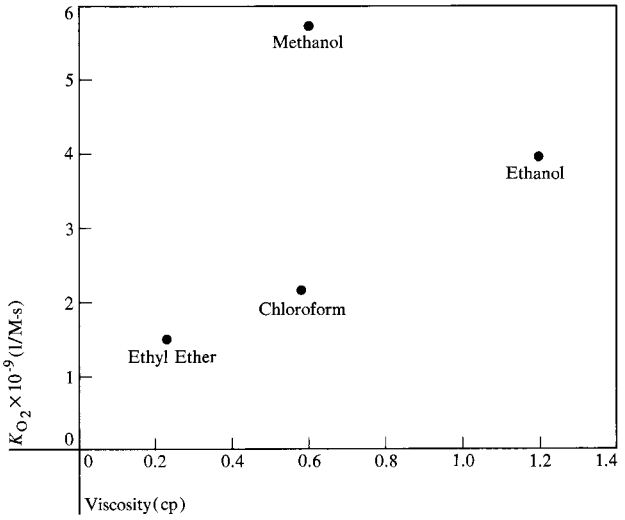

Appendix B: Calculation of dissolved oxygen

To calculate the concentration of dissolved oxygen, one needs the solubilities that can be defined in terms of the Ostwald coefficient.

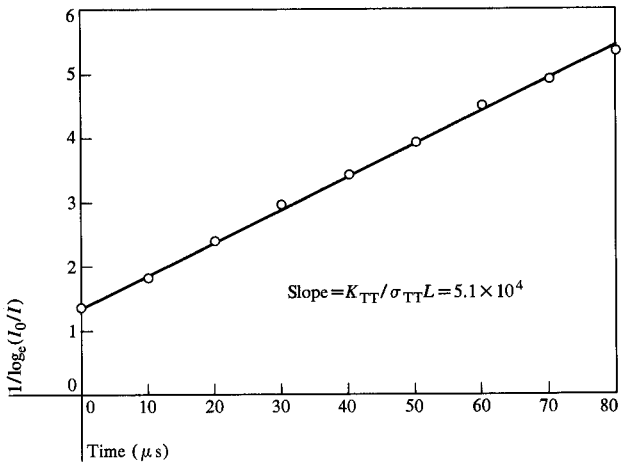

Figure A5 Data for triplet-triplet quenching in de-gassed solutions.

The Ostwald coefficient, l, is defined as the ratio of the volume of gas, V_g, absorbed at any partial pressure and temperature by the volume of liquid, V_l

$$l = V_g/V_l.$$

The number of moles of gas absorbed is

$$n = P_g V_g/RT,$$

where P_g is the partial pressure of the gas, $R = 0.0821$ l-atm/M-K is the universal gas constant, and T is the absolute temperature. Substituting Eq. (j) into Eq. (k), we calculate the molarity of dissolved gas.

$$n/V_l = P_g l/RT.$$

or, using $P_g = 0.21$ atm,

$$n/V_l = (8.5 \times 10^{-3}) l \text{ M/l}.$$

Acknowledgments

The authors are grateful to L. M. Taylor for his assistance with the experimental measurements. Thanks are due also to W. Knecht of Wright Patterson Air Force Base and R. A. Keller of the National Bureau of Standards for their many valuable discussions, and to G. Farmer and D. Wenstrand for their triplet lifetimes measurements.

References and notes

1. M. J. Weber and M. Bass, "Frequency and Time Dependent Gain Characteristics of Dye Lasers," *IEEE J. Quantum Elec.* **QE-5,** 175–188 (1969).
2. B. B. Snavely and O. G. Peterson, "Experimental Measurement of the Critical Population Inversion for the Organic Dye Laser," *IEEE J. Quantum Elec.* **QE-4,** 540–545 (1968).
3. P. P. Sorokin, J. R. Lankard, V. L. Moruzzi and E. C. Hammond, "Flashlamp Pumped Organic Dyes," *J. Chem. Phys.* **48,** 4726-4741 (1968).
4. J. B. Marling, D. W. Gregg and L. Wood, "Chemical Quenching of the Triplet State in Flashlamp-Excited Liquid Organic Lasers," *Appl. Phys. Letters* **17,** 527–530 (1970); R. Pappalardo, H. Samelson and A. Lempicki, "Long Pulse Laser Emission from Rhodamine 6G Using Cyclooctatetraene," *Appl. Phys. Letters* **16,** 267 (1970).
5. G. Burns and A. H. El Chichiny, "Laser Rate Equations (4-Level Rate Equations at High Temperatures)" IBM Research Note #NZ-38, Zürich Research Laboratory, June 26, 1964. Available on request from the library at the IBM T. J. Watson Research Center, Yorktown Heights, N.Y.
6. D. L. Stockman, "Stimulated Emission Considerations in Fluorescent Organic Molecules," *Proc. Conf. on Organic Lasers*, May 25, 1964, DDC #AD 447 468.
7. V. Evtukhov and J. K. Neeland, "Laser Devices Exploratory Investigation," Final Report, AFAL-TR-66-238, October, 1966, AD #800664.
8. B. B. Snavely and F. P. Schafer, "Feasibility of CW Operation of Dye Laser," *Phys. Letters* **28A,** 728 (1969).
9. O. G. Peterson, S. A. Tuccio and B. B. Snavely, "CW Operation of an Organic Dye Solution Laser," *Appl. Phys. Letters* **17,** 245 (1970).
10. See Appendices A and B for a more detailed discussion of oxygen quenching of triplet states.
11. R. A. Keller, "Effect of Quenching of Molecular Triplet States in Organic Dye Laser," *IEEE J. Quantum Elec.* **QE-6,** 411 (1970); see also references therein.
12. D. L. Stockman, Xerox Corporation, private communication.
13. J. P. Webb, W. C. McColgin, O. G. Peterson, D. L. Stockman and J. H. Eberly, "Intersystem Crossing Rate and Triplet State Lifetime for a Lasing Dye," *J. Chem. Phys.* **53,** 4227 (1970).
14. B. G. Huth, "Direct Gain Measurements of an Organic Dye Amplifier," *Appl. Phys. Letters* **16,** 185 (1970).
15. B. H. Soffer and J. W. Linn, "Continuously Tunable Picosecond-Pulse Organic-Dye Laser," *J. Appl. Phys.* **39,** 5859 (1968).
16. B. B. Snavely, *Proc. IEEE* **57,** 1374 (1969).
17. This entire discussion has, of course, been based on the assumption that $\xi < 1$. If the opposite is true, triplet state absorption can indeed cause early termination of the laser pulse.
18. B. B. Snavely, Eastman Kodak Research Labs., private communication.
19. R. Targ and W. B. Tiffany, "Gain and Saturation in Transverse. Flowing CO_2-N_2- He Mixtures, *Appl. Phys. Letters* **15,** 302 (1969).
20. W. Koechner, "Analytical Model of a CW Y Laser," *Laser Focus* **6,** No. 4, 37 (1970).
21. D. S. Kliger and A. C. Albrecht, "Nanosecond Excited-State Polarized Absorption Spectroscopy of Anthracene in the Visible Region," *J. Chem. Phys.* **50** 4109–4111 (1969).
22. For diffusion-controlled, collisional quenching the rate constant is given approximately by $K_Q = (8RTp/3000\eta)$ 1/M-s, where $R = 8.31 \times 10$ erg/M-deg is the universal gas constant, T is the temperature in degrees Kelvin, η is the viscosity in poise, and p is the probability that quenching occurs in a collision. For lack of more specific information, we will assume that $p = 1$. For more details see *Progress in Reaction Kinetics*, Edited by G. Porter, Vol. 4, Pergamon Press, 1967, p. 251 or I. B. Berlman, *Handbook of Fluorescence Spectra of Aromatic Molecules*, Academic Press, New York, 1965, p. 37.

Received February 10, 1971

The authors are located at the IBM Federal Systems Division, Gaithersburg, Maryland 20760.